Build Simul
https://doi.org/10.1007/s12273-020-0677-3

Assessing ventilation control strategies in underground parking garages

Afshin Faramarzi, Jongki Lee, Brent Stephens, Mohammad Heidarinejad (✉)

Department of Civil, Architectural, and Environmental Engineering, Illinois Institute of Technology, Chicago, IL, USA

Abstract

Enclosed parking garages require mechanical ventilation fans to dilute concentrations of pollutants emitted from vehicles, which contributes to energy use and peak electricity demand. This study develops and applies a simulation framework combining multi-zone airflow and contaminant transport modeling, fan affinity laws, and realistic assumptions for vehicle traffic patterns and carbon monoxide (CO) emissions to improve our ability to predict the impacts of various ventilation control strategies on indoor air quality and fan energy use in parking garages. The simulation approach is validated using measured data from a parking garage case study and then applied to investigate fan energy use, peak power demand, and resulting CO concentrations for four different ventilation control strategies in a model underground parking garage under a variety of assumptions for model inputs. The four ventilation control strategies evaluated include one simplistic schedule (i.e., Always-On) and three demand-based strategies in which fan speed is a function of CO concentrations in the spaces, including Linear-Demand Control Ventilation (DCV), Standardized Variable Flow (SVF), and a simple On-Off strategy. The estimated annual average fan energy consumption was consistently lowest with the Linear-DCV strategy, resulting in average (± standard deviation) energy savings across all modeled scenarios of 84.3%±0.4%, 72.8%±3.6%, and 97.9%±0.1% compared to SVF, On-Off, and Always-On strategies, respectively. The utility of the framework described herein is that it can be used to model energy and indoor air quality impacts of other parking garage configurations and control scenarios.

Keywords

carbon monoxide,
demand control ventilation,
energy efficiency,
indoor air quality,
underground parking garage

Article History

Received: 20 January 2020
Revised: 22 May 2020
Accepted: 14 June 2020

1 Introduction

Automobile parking garages require ventilation to dilute contaminants generated by vehicles operating within them (Zhao et al. 2018; Liu et al. 2019). Partially open parking garages, which are usually constructed above-grade over structural decking, commonly have at least three sides open to the outdoor environment to allow for natural ventilation to dilute contaminants without the use of mechanical fans. Conversely, fully enclosed parking garages, which are often located underground, require mechanical ventilation, which is most often achieved using either centrifugal fans to exhaust contaminants or axial fans to supply ventilation air (ASHRAE 2011). The use of ventilation fans in underground parking garages contributes to energy use and peak electricity demand, both of which will vary in magnitude depending on system design, equipment type, and control strategy utilized (Chan et al. 1998; Chan and Chow 2004; Gil-Lopez et al. 2014).

Maximum allowable contaminant concentrations are commonly used to establish required ventilation rates for underground garages. Internal combustion engines emit a variety of contaminants including particulate matter, volatile organic compounds (VOCs), oxides of nitrogen (NO_x), carbon dioxide (CO_2), and carbon monoxide (CO) (Abdel-Rahman 1998). CO is most commonly used to determine ventilation rates because of its known acute and chronic health effects, it is regulated by numerous governing bodies and standards organizations, and it is relatively inexpensive to measure compared to other contaminants (Marr et al. 1998; Gil-Lopez et al. 2014; Zhao et al. 2017). For example, the American Conference of Governmental Industrial Hygienists (ACGIH) recommends a maximum 8-hour CO

E-mail: muh182@iit.edu

exposure of 25 ppm (ACGIH 1998); U.S. Environmental Protection Agency (EPA) maintains an acceptable 1-hour peak exposure of up to 35 ppm and an 8-hour of exposure up to 9 ppm in ambient air (EPA 2000); and the Occupational Safety and Health Administration (OSHA) defines an 8-hour permissible exposure limit (PEL) of 50 ppm (OSHA 2012).

Accordingly, ASHRAE Standard 62.1-2019 requires parking garages to have a minimum constant exhaust rate of 3.7 L/s per m^2 of floor area (ASHRAE 2019), while the 2015 International Mechanical Code (IMC) allows for adjustable speed systems that are capable of producing a ventilation flow rate of 3.8 L/(s·m^2), but must maintain a constant minimum ventilation rate of 0.25 L/(s·m^2) (ICC 2015). Conversely, the California Energy Code requires a higher minimum ventilation rate of 0.75 L/(s·m^2) at all times (Title 24 2013). The 2015 IMC also allows adjustable speed systems to operate on an intermittent basis as long as they are automatically controlled with CO and NO_2 sensors. CO-based demand control ventilation (DCV) strategies, in which the ventilation airflow rate varies based on CO concentrations in the space, have been shown to be effective in conserving fan energy while maintaining CO concentrations below defined threshold levels (Lorenz 1982; Krarti et al. 1998; Cho and Jeong 2013). However, the trade-offs between resulting contaminant concentrations and fan energy (and peak demand) savings of different approaches to CO-based DCV have not been investigated in detail. For example, previous studies have compared constant volume systems to on/off control (i.e., with fan operation started and stopped based on input from CO sensors) or variable air volume (VAV) control with multi-speed fans (Krarti et al. 1998; Ayari et al. 2000; Krarti and Ayari 2003). The use of variable frequency drives (VFDs) could allow for fan speed adjustments with finer resolution in response to contaminant concentrations, but to our knowledge they have not yet been studied in depth.

Therefore, this study provides a comprehensive assessment of various ventilation control strategies for fan operation in underground parking garages. While some prior studies have used computational fluid dynamics (CFD) simulations to investigate the distribution of contaminants in parking garages in great detail (Krarti and Ayari 2003; Duci et al. 2004; Aminian et al. 2018a, b), here we use a multi-zone airflow model (CONTAM (Dols and Polidoro 2015)) based on an actual parking garage to evaluate the impacts of control strategies on fan energy consumption, fan peak electricity demand, and resulting CO concentrations in modeled garages. CONTAM has been used successfully for somewhat similar studies of CO transport in residential parking garages and from portable generators in attached garages (Wang et al. 2014; Dols et al. 2016; Emmerich et al. 2016; Emmerich and Dols 2016). Although CONTAM is able to solve the Navier-Stokes equations for CFD modeling (via the CFD0 module), this study instead uses the simpler multi-zone modeling approach in CONTAM, which solves a set of non-linear mass conservation equations to estimate pressure distributions in each zone and to calculate the airflow through the zones. This tool was chosen because it allows for rapid assessment of contaminants under different ventilation control network assumptions. The details of the governing equations, numerical solvers, and other relevant information are available in the CONTAM manual and existing literature (Dols and Polidoro 2015; Qi et al. 2015; ASHRAE 2017).

Although there is a growing body of literature focused on DCV applications in office and residential buildings (Demetriou and Khalifa 2009; Hong and Fisk 2010; Laverge et al. 2011; Hesaraki and Holmberg 2015; Guyot et al. 2018), DCV applications in parking garages remains an understudied, albeit promising, area for building simulation and energy efficiency improvements. For example, in one study, CONTAM was used to assess energy savings of using four different demand control strategies in residential buildings (Laverge et al. 2011). The four strategies included (i) airflow adjustment in vent holes based on relative humidity, (ii) occupant-based control of exhaust fans, (iii) regulating supply ventilator openings based on the CO_2 concentration, and (iv) a combination of the three strategies. The simulation results estimate a potential energy savings ranging from 25% to 60% compared to the baseline. Another study modeled different demand control ventilation strategies to control VAV systems in newly built homes using IDA Indoor Climate and Energy software (Hesaraki and Holmberg 2015). These strategies aimed at varying the ventilation rate from its standard levels during unoccupied hours to meet indoor air quality requirements while saving up to 30% on electricity consumption. Another recent study conducted a comprehensive literature review on various examples of DCV in residential buildings (Guyot et al. 2018). However, none of the reviewed studies have considered the implications of using DCV in parking garages, which presents a knowledge gap that this study aims to address.

2 Methods

To evaluate different ventilation control strategies, this study first developed a simulation framework that utilizes a variety of realistic methods and assumptions for key parameters. Figure 1 illustrates three steps used in this study to validate and demonstrate the developed framework. In Step 1, described in Section 2, a series of realistic methods and assumptions and methods are developed to establish the framework. In Step 2, described in Section 3, the developed framework is validated using CO concentration measurements from a real parking garage with actual vehicle traffic data.

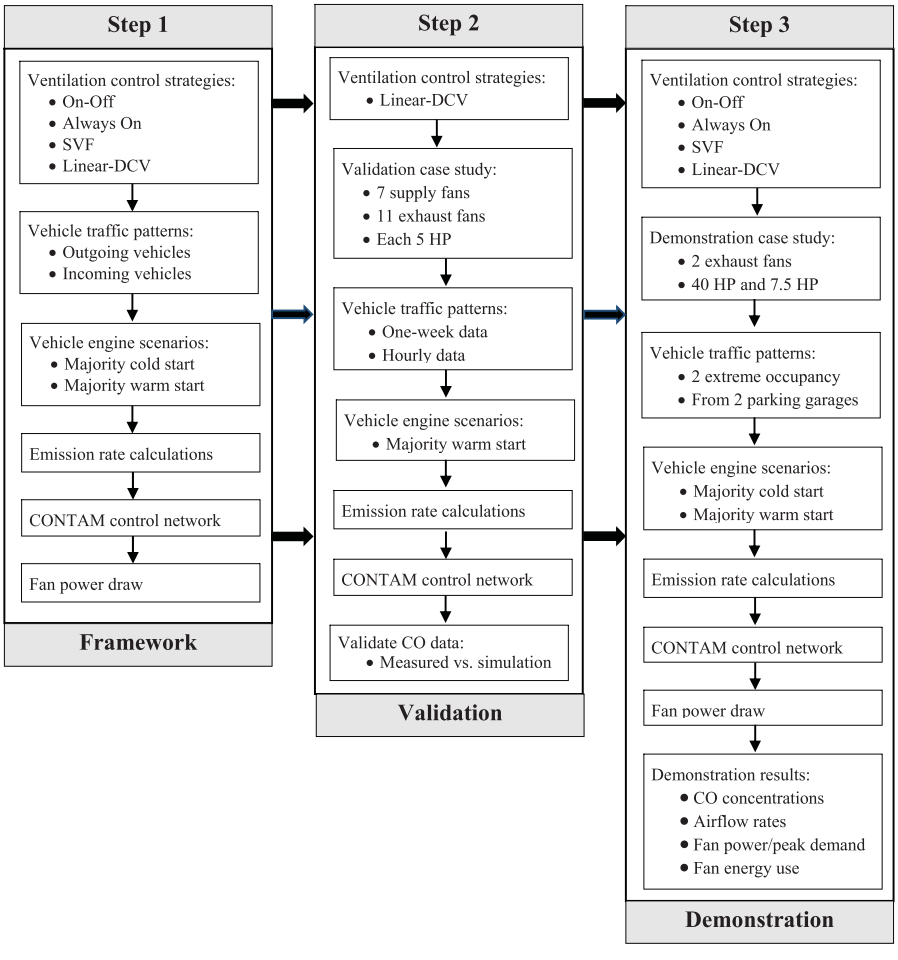

Fig. 1 The steps developed in this study to validate and demonstrate the model framework

In Step 3, described in Section 4, the developed framework is applied to investigate the impacts of four different ventilation control strategies in a case study parking garage using two models and various assumptions for the model inputs described in Step 2. The next sections describe the ventilation control strategies that were evaluated and the detailed inputs that were used to inform a realistic multi-zone model in CONTAM.

2.1 Ventilation control strategies

Figure 2 depicts four different ventilation control strategies evaluated in this study, in which fan motor speed is shown as a function of simultaneous CO concentrations in the garage. The simplest strategy, Always-On, operates the fan at 100% of maximum speed during operating hours regardless of the CO concentration. In the On-Off strategy, the fan operates at 100% of maximum speed only when CO concentrations in any zone reach a threshold of 25 ppm; the fan does not operate when CO concentrations are below 25 ppm. This approach is commonly used in the industry, and a threshold concentration of 25 ppm was used based on the aforementioned ACGIH recommendations (many equipment manufacturers recommend using 25 ppm in practice as well). The Standardized Variable Flow (SVF) strategy is also commonly used in the industry as an energy saving approach whereby the fans operate at 50% of maximum speed until CO concentrations reach 25 ppm, at which point they increase

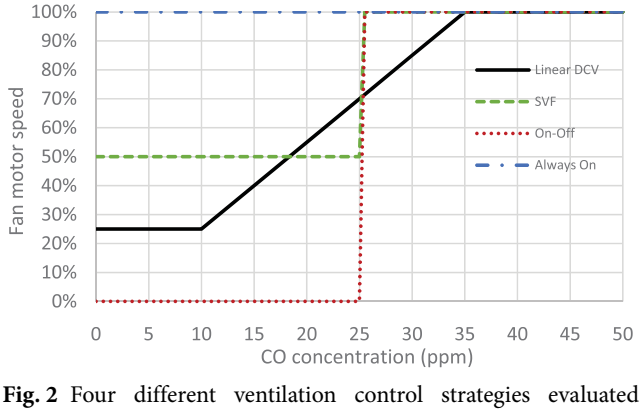

Fig. 2 Four different ventilation control strategies evaluated herein

to 100% of maximum speed. Finally, the Linear-DCV strategy assumes that VFDs control fan speed from a minimum of 25% of maximum speed until the average CO concentration in all zones reaches 10 ppm, at which point the fan speed increases linearly until the average CO concentration reaches 35 ppm (i.e., by 3% for every additional 1 ppm of average CO concentration in the space); and the fans operate at maximum speed when average CO concentrations are 35 ppm and above. The nature of the Linear-DCV control strategy is inspired by CO_2-based DCV sometimes used in commercial buildings (Lu et al. 2011).

2.2 Vehicle traffic patterns

Previous studies have noted that the number of operating cars inside parking garages at a given time commonly varies from 3% of the total parking capacity in shopping areas to up to 20% in stadiums for sporting events (Krarti et al. 1998). Here we use actual vehicle occupancy patterns from transaction data obtained from two real parking garages in the U.S. Traffic Schedule 1 is for a shopping center and Traffic Schedule 2 is for an office building. We use these two different traffic schedules in the same garage model to test the sensitivity of the model to varied inputs. The operating hours (i.e. the time that fans in a parking garage are operating) of the parking garage with Traffic Schedule 1 are from 4 a.m. to 10 p.m. on weekdays, from 7 a.m. to 10 p.m. on Saturdays, and from 9 a.m. to 10 p.m. on Sundays. For the parking garage with Traffic Schedule 2, the operating hours are from 5 a.m. to 2:30 a.m. on weekdays and 6:30 a.m. to 3 a.m. on weekends. Figure 3 shows the normalized occupancy schedules for incoming and outgoing vehicles for both parking garages. Normalized occupancy is defined as the real occupancy per hour divided by the number of zones in the garage and a defined multiplier that accounts for incoming and outgoing vehicles separately. Normalized occupancy is used because CONTAM accepts only normalized states between zero and one for control algorithms. Since we had access only to the total garage occupancy data and not the zone level occupancy, we assume that incoming and outgoing vehicles are uniformly distributed throughout the different zones (i.e., the traffic patterns are considered the same for all zones). Although the occupancy schedule of any garage depends on the type of garage, its location, season, day of

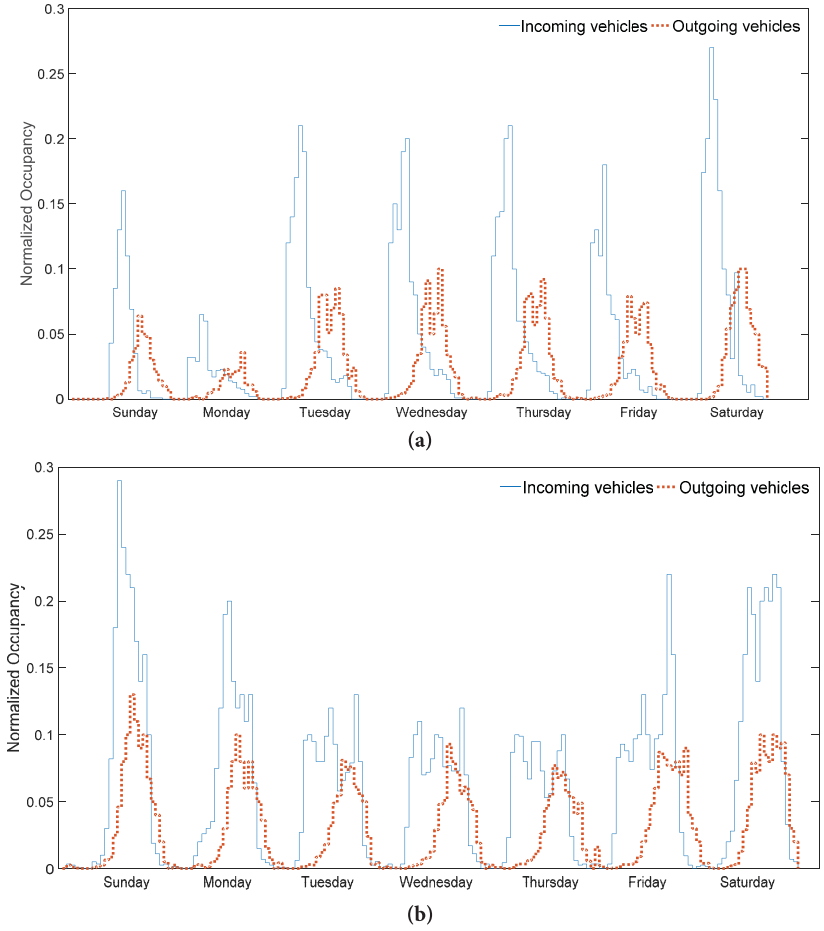

Fig. 3 Normalized vehicle occupancy patterns for (a) Traffic Schedule 1 and (b) Traffic Schedule 2

the week, and other factors, the presented annual average occupancy data provides a realistic example of traffic patterns in underground parking garages.

The operating time of a vehicle in a parking garage (i.e., the time that a vehicle spends operating in a parking garage) is highly dependent on the size and layout of the garage and number of incoming and outgoing vehicles at a given time. Operating times commonly vary from as little as 60 s to as much as 600 s, depending on a number of factors, but the average duration spent in garages typically ranges from 60 s to 180 s (ASHRAE 2011). Based on these observations and our real occupancy data, we assume that the average operating time of incoming and outgoing vehicles is 180 s and 60 s, respectively. In other words, we assume that it takes 3 minutes to find a parking spot and 1 minute to leave the garage. Because our defined operating schedule in CONTAM would assume that the normalized occupancy values in Figure 3 would apply for the entire 1-hour duration, the normalized occupancy data is multiplied by 0.05 (i.e. 3 min/60 min) for incoming vehicles and by 0.0167 (i.e. 1 min/60 min) for outgoing vehicles. For both traffic schedules, occupancy pattern data from the week with the highest recorded occupancy was selected for implementation in CONTAM simulations to represent worst case vehicle emissions scenarios. For simplicity, this weeklong pattern is also assumed to represent all 52 weeks of a year to estimate annual energy impacts.

2.3 Vehicle engine scenarios

The number of operating combustion engine vehicles and CO emission quantities from each vehicle are among main factors to determine the minimum required ventilation rate for underground parking garages (Krarti et al. 1998). CO emission rates depend on whether the engine is operating in "cold start" or "warm start" conditions. "Cold start" conditions exist when a vehicle is started after it has been sitting for a long period of time (i.e. after a soak time of 12 hours or more) and thus has a high CO emission rate upon ignition (Gao and Johnson 2009). Conversely, "warm start" conditions exist when a vehicle is started after sitting for a shorter period of time (i.e. after a soak time of less than 12 hours), and thus the CO emission rate upon ignition is lower than the cold start condition. This study assumes two engine start scenarios for each traffic schedule: (1) majority cold start conditions, which represents a hypothetical worst case scenario in which an assumed 80% of vehicles emit CO in the cold start condition, and (2) majority warm start conditions, in which a more realistic distribution of engine start conditions is assumed based on actual garage data. Assumed CO emission rates for each condition are explored in more detail in Section 2.4. Moreover, although the data in Figure 4 do not distinguish between electric vehicles (EV), which do not emit CO, and vehicles with combustion engines, we assume for simplicity that all vehicles have combustion engines. We also assume that most vehicle movement in parking garages is in low gear at low speeds (i.e., 24 km/h).

2.4 Emission rate calculations

CO emissions from engine starts are a highly dynamic process that should be accounted for in modeling. Additionally, the ambient temperature also influences CO

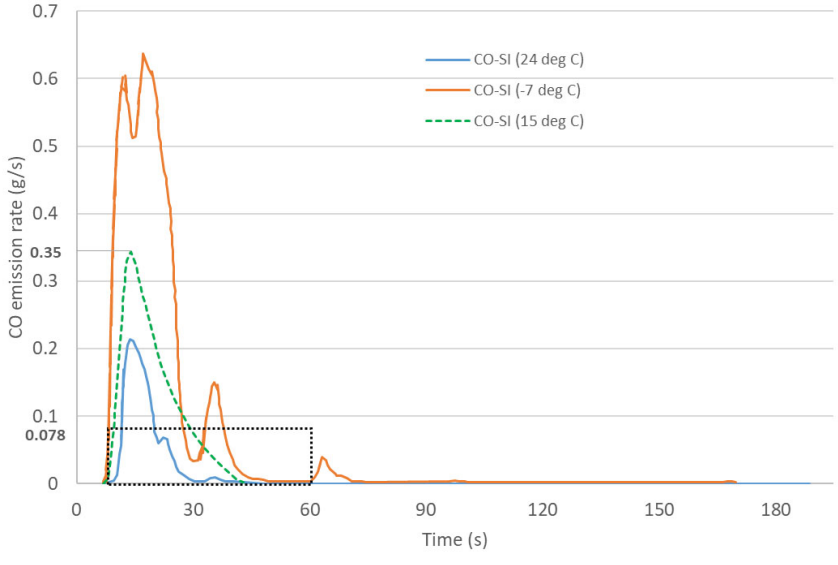

Fig. 4 Example of CO emissions profile of a spark ignition engine for a typical passenger vehicle during cold start conditions at varying temperatures (figure is reproduced from (Bielaczyc et al. 2013))

emissions, with colder temperatures leading to higher CO emissions during both "cold starts" and "warm starts" (ASHRAE 2011). For example, Figure 4 shows an example of the time-varying CO emission rate from a cold start of a modern spark ignition engine for a typical passenger vehicle under two ambient temperatures: −7 °C and 24 °C (Bielaczyc et al. 2013). At both temperatures, there is an initial CO emission peak within the first 30 seconds, followed by a decay throughout the remaining 30–60 seconds. Additionally, ambient temperature has a considerable effect on the emission peak, with cold temperatures resulting in a peak emission rate that is approximately three times higher than the warmer condition tested.

This study assumes the temperature of the case study parking garage is a constant 15 °C. The time-varying CO emission profile of a spark ignition engine at this temperature can thus be estimated by interpolating between the two curves in Figure 4 (i.e., the green dotted line, interpolating between −7 °C and 24 °C). Then, the time-varying CO emission profile is estimated using equivalent 1-min average emission rates. Assuming that it takes 1 min on average for a vehicle to leave the parking garage, the dotted green triangle can be considered to be the same as the area of the dotted black rectangle. Using numerical integration, the mass of CO emitted in the first 60 seconds is estimated to be 10.2 g and 1.94 g at −7 °C and 24 °C, respectively. Linear interpolation is used to estimate the mass of CO emitted during a cold start at 15 °C to be 4.3 g. Assuming this mass is emitted during a 1-min interval, the emission rate is thus 4.3 g/min; however, we apply an additional 10% factor of safety to account for slight nonlinearities in the emission profile and thus use a cold start emission rate of 4.7 g/min (i.e., 4.3 × 1.1).

For warm start conditions, we assume that the average CO emission rate for a passenger vehicle with a running internal combustion engine is 0.13 g/min, which is taken from the California Air Resources Board (CARB) database of Emission FACtors (EMFAC) (CARB 2017a,b) assuming a vehicle speed of 24 km/h and an average vehicle vintage of 2010. Thus, the warm start CO emission rate is assumed to be less than 3% of the average cold start CO emission rate. Therefore, for the majority cold start scenario, in which 80% of vehicles are assumed to emit CO in the cold start conditions, the average CO emission rate is assumed to be 3.76 g/min (i.e., 4.7 g/min × 80%) and the hot start emissions are assumed to be negligible.

Conversely, the majority warm start scenario assumes a distribution of CO emission factors based on an assumed distribution of vehicle soak times (recall that a soak time refers to the time that a vehicle's engine is off). Figure 5 presents a soak time distribution of vehicles from a randomly selected day of transient vehicle entrance and exit data from Traffic Schedule 2 (only data from this garage was available, so the distribution is assumed to be the same for both garages). The majority of vehicles (i.e., 85%) experience a soak time of between 1 and 4 hours, meaning they experience warm start conditions. For simplicity, we considered the remaining 15% of vehicles to be starting from cold start conditions (i.e., from 5 hours to the end of the distribution). Since this scenario is based on real data, it is considered a more realistic day-to-day operational scenario.

CARB provides a relationship between normalized CO emission rates versus soak time for recent passenger vehicles equipped with catalytic convertors (CARB 1997). The data in CARB allow for estimating CO emission rates for different soak times by applying a correction factor for varying bins of soak times. Table 1 presents the average CO emission correction factor based on the CARB data for the first 4 hours of soak time. This study estimates the CO emission correction factor provided in Table 1 for the different soak time distribution bins in Figure 5.

Based on the data in Table 1 and the soak time distribution

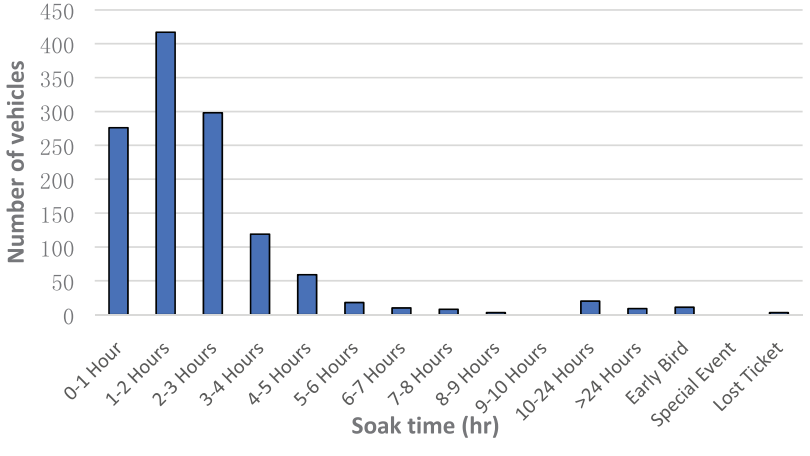

Fig. 5 Soak time distribution used for both traffic schedules

Table 1 Average CO emission correction factor for different soak time bins

Soak time (min)	Average correction factor
0–60	0.30
60–120	0.66
120–180	0.75
180–240	0.78

in Figure 5, Eq. (1) calculates a Weighted Correction Factor (WCF) for the CO emission rate in the first 4 hours of soak times for the 85% of vehicles that are assumed to start under warm start conditions by multiplying the weighted vehicle occupancy from Figure 5 by the average correction factor from Table 1 for the first 4 hours of soak time.

$$\begin{aligned} \mathrm{WCF}_{\text{warm start}} &= \sum_{i=1}^{4}\left(\text{weighted vehicle occupancy}\right)_i \\ &\quad \times \left(\text{average correction factor}\right)_i \\ &= 0.2\times 0.3 + 0.33\times 0.66 + 0.23 \\ &\quad \times 0.75 + 0.095\times 0.78 = 0.5 \end{aligned} \tag{1}$$

Accordingly, we assume that the 15% of vehicles that start in cold start conditions have an average CO emission rate of 4.7 g/min (as described previously) and that the 85% of vehicles that start in warm start conditions have an average CO emission rate of 0.5 × 4.7 g/min.

2.5 CONTAM control network model

Although many previous studies have used CONTAM for airflow modeling, only a limited number of studies have used the CONTAM control network functions in detail (Laverge et al. 2011; Dols and Polidoro 2015). The control functions in CONTAM include different proportional controls (P, PI), limit controls (upper, lower) and switches (upper, lower). Limit controls provide the ability to send an error signal ranging from 0 to 1 as an output based on the difference between two input signals. Limit switches can send a binary signal based on this difference. The control functions and logic that we used are explained in more detail in Section 3.

2.6 Fan power draw

Fan laws relate the variables for any dynamically similar series of fans, as shown in Eqs. 2(a) and 2(b) (ASHRAE 2008). Variables include fan size D, speed N, gas density ρ, airflow rate Q and power W, and subscripts 1 and 2 refer to the conditions at which the fan is operating:

$$Q_1 = Q_2 \times \left(D_1 / D_2\right)^3 \left(N_1 / N_2\right) \tag{2a}$$

$$W_1 = W_2 \times \left(D_1 / D_2\right)^5 \left(N_1 / N_2\right)^3 \left(\rho_1 / \rho_2\right) \tag{2b}$$

To estimate the power draw of a fan operating at various speeds (or airflow rates), we utilize known fan curve relationships. The fan curves for the demonstration case study were generated using actual measurements of fan power draw at different increments of fan speed taken from the parking garage on which our model is based. For the points for which we did not have data, we used the fan affinity laws in Eqs. 2(a) and 2(b). For the validation case study's fan curves, we extracted the power draw data corresponding to 0%, 50%, and 100% of maximum motor speed from the fan information of mechanical drawings provided by the designer. Then, for the points on the curve in between these fan speeds we again used fan affinity laws to generate the data based on these three points. More detail on measured fan curve data are provided in the following sections.

3 Validation study

To validate the simulation strategy described in Section 2, this study first compares the resulting CO concentrations calculated in CONTAM with actual measured CO concentration data collected from a real parking garage operating with just one of the aforementioned control strategies (Linear-DCV). The validation parking garage has a floor area of approximately 10,590 m^2. The space is equipped with 7 supply fans and 11 exhaust fans, each requiring 5 HP of fan power. The maximum flow rate of the exhaust and the supply fans are 9.0 m^3/s (19,000 cfm) and 3.8 m^3/s (8,100 cfm), respectively. This study collected data on the number of vehicles and CO concentrations for the week of August 22, 2019 to August 28, 2019. The outdoor air temperature varied from 12.8 °C to 25.6 °C, and the average temperature was about 18.7 °C. This study assumed the parking garage in the simulation was a constant 20 °C for simplicity. Figure 6 illustrates the normalized incoming and outgoing vehicles for this case study parking garage. These are actual hourly traffic for this week. In addition, the soak distribution schedule in this case follows Figure 5 and Table 1 because the traffic schedule is from the same garage.

Figure 7 shows the measured power draw versus the fan speed for both the exhaust and supply fans, measured at various fan speed intervals. Fan affinity laws were used to fit a fan curve based on these measured data for fan speeds in between those shown in Figure 7. Additionally, the fan power draw measurements indicate that the supply fans and exhaust fans have different power draw characteristics because the types of fans in both systems are different; a

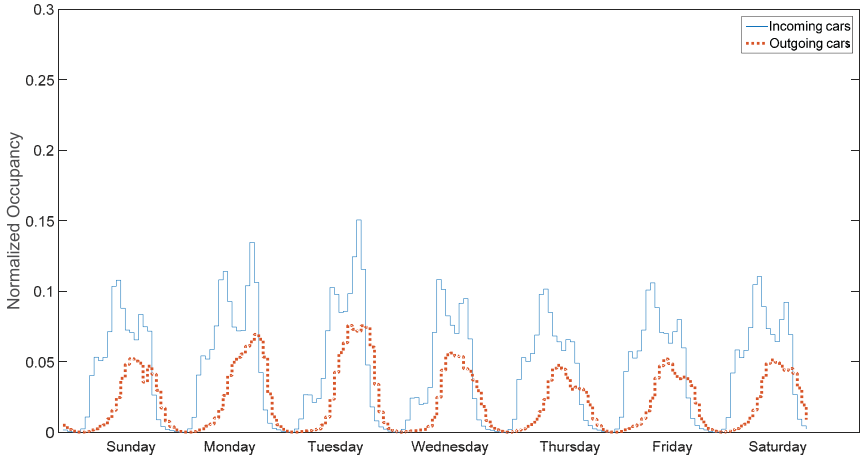

Fig. 6 Normalized vehicle traffic schedule in the parking garage used for validation

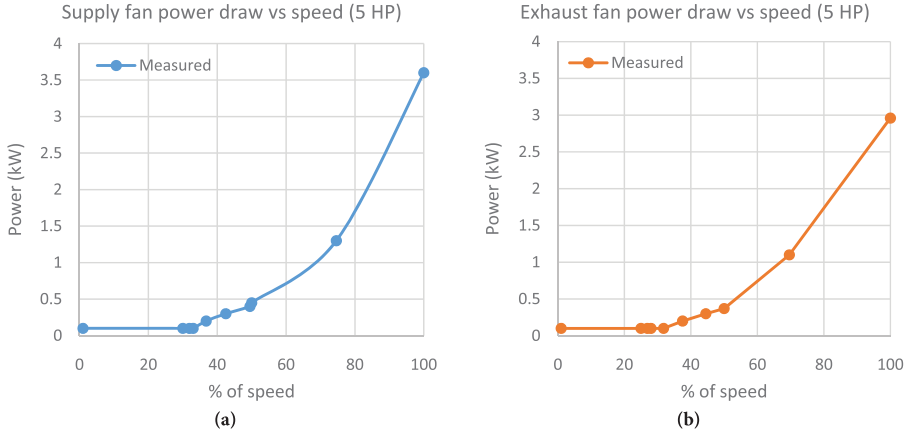

Fig. 7 Measured power draw with respect to fan motor speed in the validation parking garage case study: (a) supply fan and (b) exhaust fan

vane axial type fan is used in the supply fans and a sidewall propeller type is used in the exhaust fans.

To represent the Linear-DCV system installed in the parking garage in the CONTAM control network, Figure 8 illustrates the schematic of zones along with the layout of sensors in the validation model. This parking garage has 13 zones on the upper floor and 18 zones on the lower floor. The installed CO sensors were NES 200 series, with a range of 0–250 ppm, resolution of ±3 ppm, repeatability of ±3% of reading, and a response time of t_{90} < 50 seconds (NES 2020). The sensors were installed at a height of 1.5 m above the floor, and each specified zone in the garage was equipped with a sensor, labeled as P1 to P31 in Figure 8.

Figure 9 depicts the control network implemented in CONTAM for the Linear-DCV strategy in which each zone concentration is defined as an input to the control network. The control network calculates the average CO concentration across all zones in the first floor and compares it with the low threshold concentration (10 ppm); the difference between these values is treated as the "error." The comparison also sets the upper limit control and sends an output signal. Next, the slope of the Linear-DCV strategy is multiplied by the error provided by the upper limit control to specify the required increase in fan speed at the observed CO concentration. Subsequently, the baseline airflow (i.e., 25% of maximum speed) is added to the output to provide the total airflow needed based on the Linear-DCV strategy. Finally, to avoid airflow exceeding 100% of the fan motor speed, the total airflow provided by the network is checked and limited to the maximum airflow rate of the fan.

Figure 10 shows a comparison between the simulated CO concentrations and the measured CO concentrations during the validation week using the assumption of majority warm start conditions. The validation uses the measured CO concentration data, which were collected in zones of P16, 17, 22, 23, 28, and 29 of the actual parking garage with a measurement interval of 10 minutes. We validated our model based on these six zones since they represented some of the highest peak occupancy and CO levels. As shown in Figure 10, the simulation results are in good agreement with

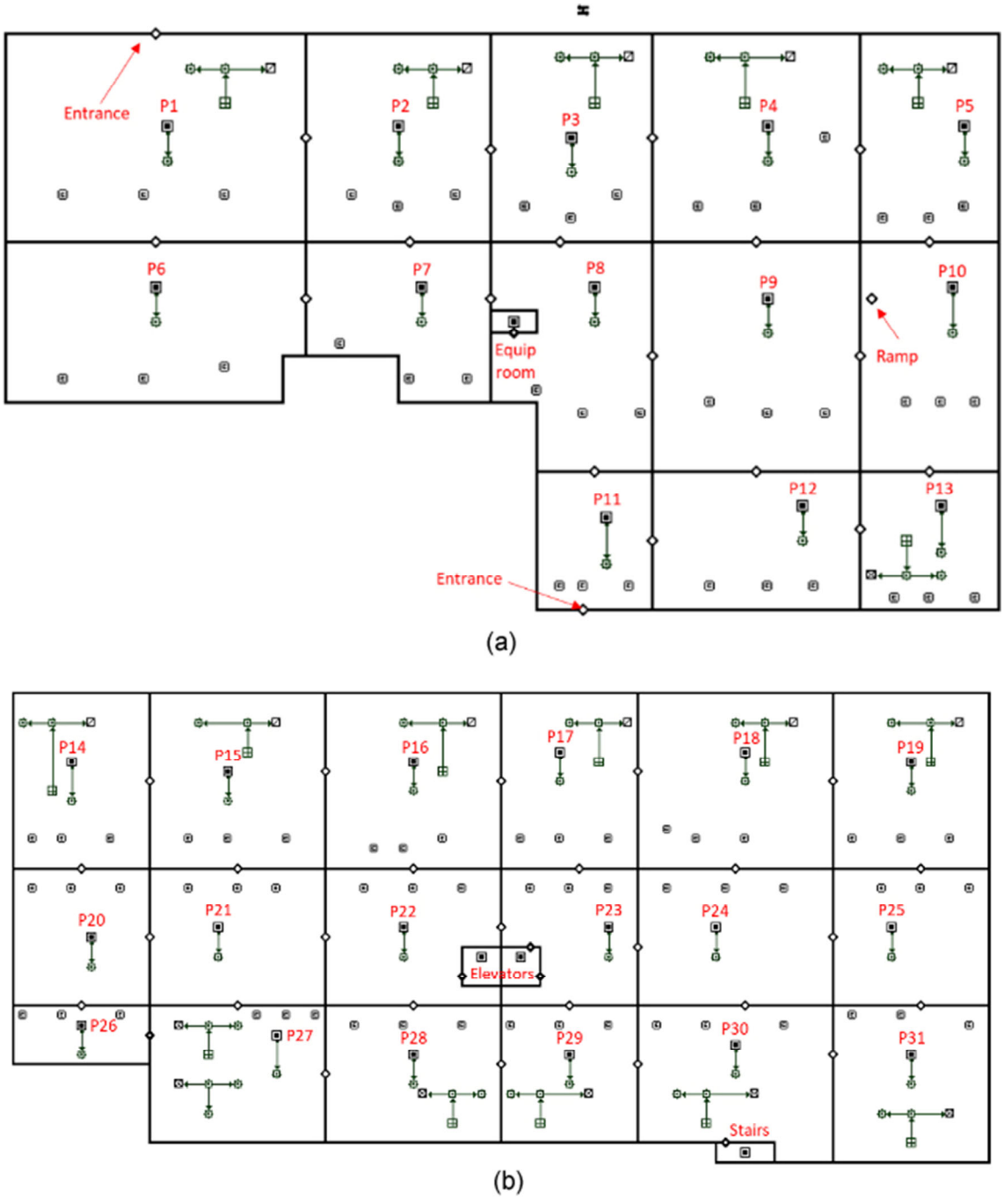

Fig. 8 Schematic of zones and CO sensors in CONTAM: Validation model (a) upper floor and (b) lower floor

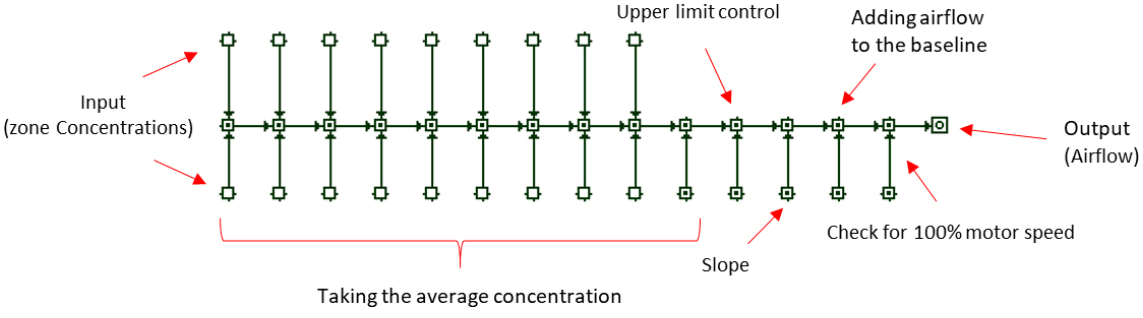

Fig. 9 Control network implemented in CONTAM for Linear-DCV

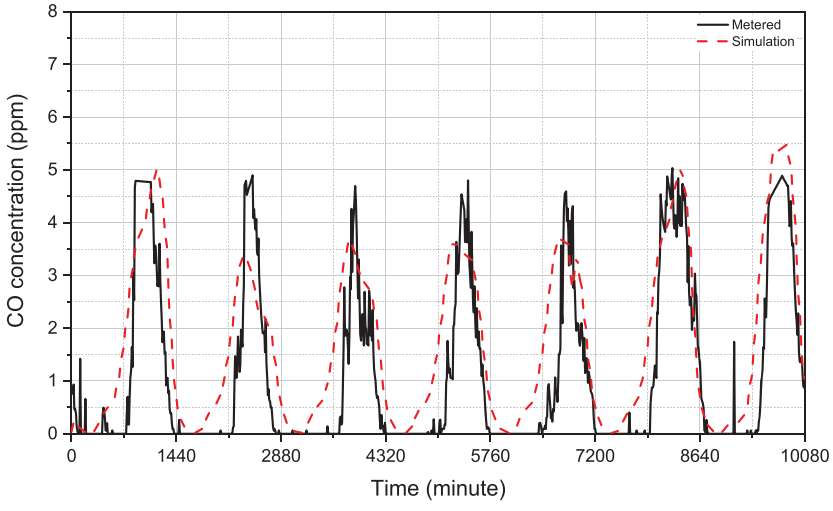

Fig. 10 Time-varying simulated and measured CO concentrations averaged across six zones of the validation parking garage (P16, P17, P22, P23, P28, and P29)

the measured results. It is observed that both simulation and measurement results follow similar CO patterns and peak times in each day.

Figure 11 quantifies the correlation between the simulation and measurement results, resulting in an R^2 = 0.78. Figure 11 also shows a polynomial regression line with 95% confidence interval prediction band. The maximum difference between the simulation and measured data is ~3 ppm, which could be attributable to sensor accuracy, sub-hourly extreme traffic, differences in measured versus modeled ventilation rates, and/or the presence of vehicles with higher CO emissions.

The results of this validation study demonstrate the utility of the proposed framework and specifically the control network implemented in CONTAM. Consequently, with the use of this developed framework, it is possible to implement a range of various assumptions to assess performance of different control ventilation strategies.

4 Demonstration study

Section 4 assesses the impacts of various ventilation control strategies and traffic patterns on resulting CO concentrations, energy use, and peak demand in a separate demonstration parking garage case study. The demonstration case study is an actual two-story underground parking garage with a floor area of approximately 8,700 m^2 as a case study to evaluate different ventilation control strategies. The garage

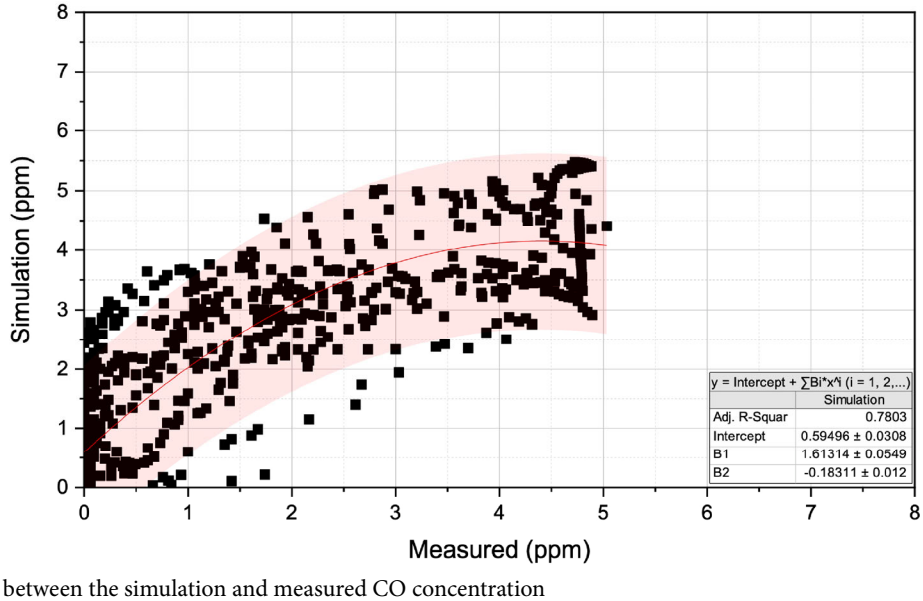

Fig. 11 Correlation between the simulation and measured CO concentration

has two exhaust fans of 7.5 HP and 40 HP to serve the upper and lower floors of the garage. The 40 HP fan serves both floors while the 7.5 HP fan only serves the upper floor due to the larger floor area of this floor compared to the lower floor. According to the manufacturer, the maximum airflow rates of the 40 HP and 7.5 HP fans are 26.4 m^3/s (56,000 cfm) and 6.6 m^3/s (14,000 cfm), respectively, providing a total maximum of 33 m^3/s when operating together. The fans were designed and selected based on the International Mechanical Code (IMC) requirement of being capable to provide 3.8 $L/(s \cdot m^2)$ (0.0038 $m^3/(s \cdot m^2)$ × 8700 m^2 = 33.06 m^3/s).

Figure 12 shows a schematic of the case study parking garage comprising 13 zones on the upper floor (Figure 12(a)) and 10 zones on the lower floor (Figure 12(b)). Each zone (illustrated with a "P" in Figure 12) is assumed to be equipped with a CO sensor and is associated with an assumed traffic pattern (described in more detail in Section 2.2). The CONTAM model entails one large entrance opening for vehicles and an internal ramp which connects the two floors to each other.

Because we have already shown the Linear-DCV control network logic in the validation section, in this section we depict only the SVF and On-Off control networks, as shown in Figure 13. For the SVF strategy, each zone CO concentration is compared to its threshold (i.e., 25 ppm)

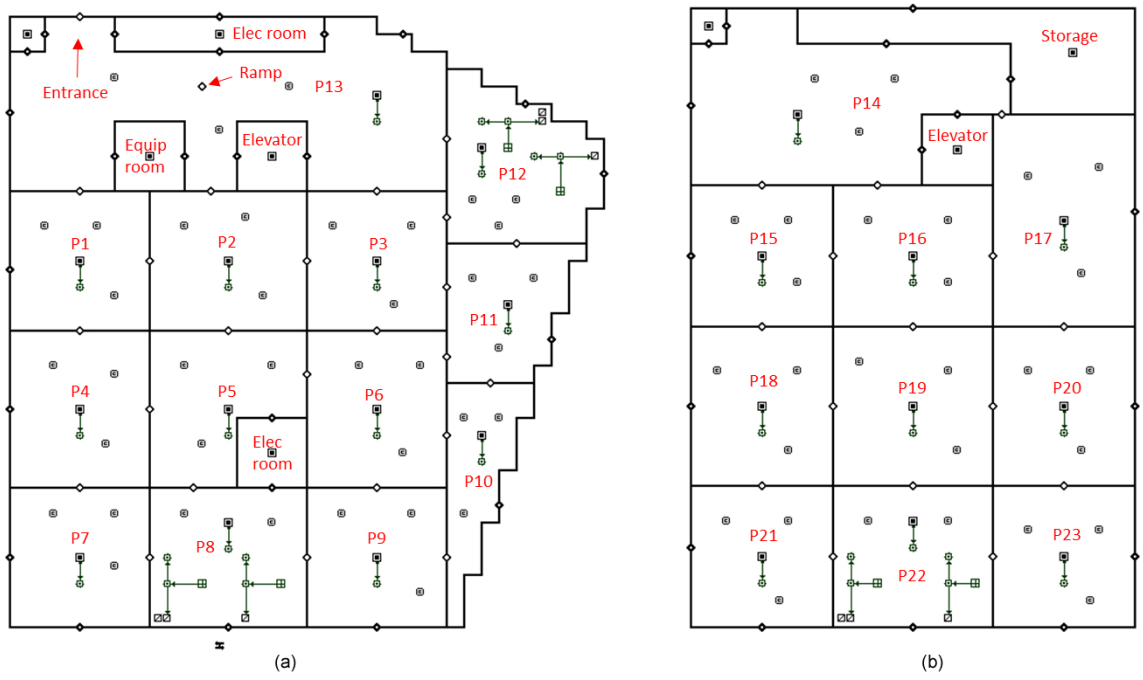

Fig. 12 Schematic of zones and CO sensors in CONTAM: Case study model: (a) upper floor and (b) lower floor

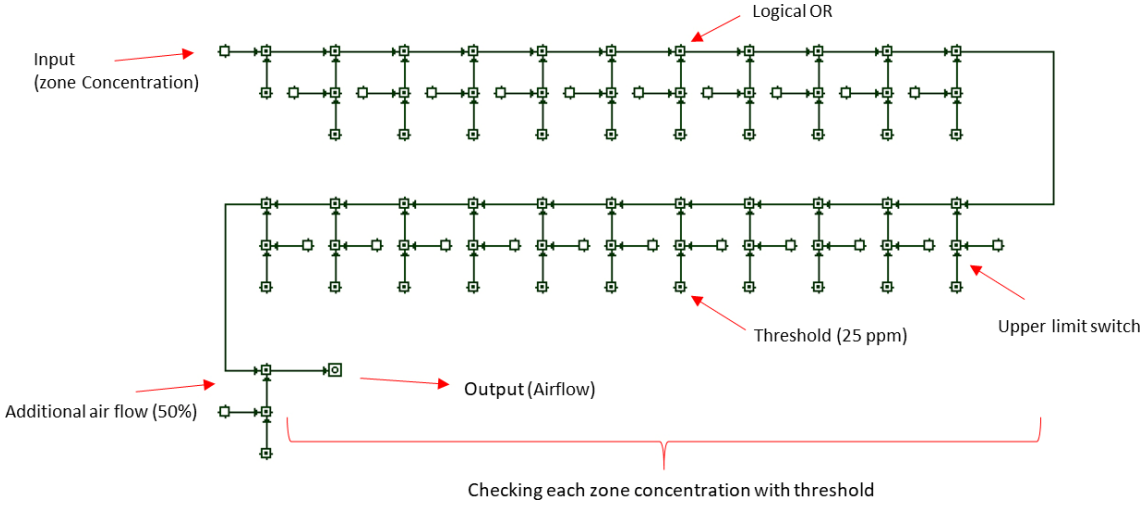

Fig. 13 Control network implemented in CONTAM for SVF or On-Off control strategies

and then a binary signal is sent to output. An output signal of 0 indicates keeping the fan off and an output signal of 1 indicates switching the fan to 50% of its maximum capacity. This configuration is implemented in series for all zones, meaning that if there is at least one zone with CO concentration above 25 ppm, the binary signal will be 1 and the fan will be set to 50% of its maximum motor speed. Before sending the output signal to the actuator, an additional baseline airflow of 50% of maximum capacity is added to provide the final output. Consequently, the SVF control network continuously provides 50% of its maximum motor speed when the output signal is 0 and reaches to 100% of its maximum capacity when the output signal is 1. The control network for the On-Off strategy follows a similar logic as the SVF control network, with the only differences including redefining the binary signal of 1 to set the fan to 100% of its full capacity and removing the baseline airflow. This redefinition allows the fans to operate at 100% capacity if the CO concentration in any zone exceeds 25 ppm and to be turned off when the CO concentration is below 25 ppm in all zones.

For each time step in the model, fan power draw is calculated as a function of fan speed for both the 7.5 HP and 40 HP fans (Figure 14). As mentioned, the fan curves in Figure 14 were generated by fitting a curve through data from actual measurements taken from the parking garage on which our model is based. The measurement was accomplished by varying fan frequency, which is linearly related to fan speed. Then, fan speed is related to fan power draw by the fan laws in Eq. 2(b). Frequency variations occur in 5 Hz intervals from 10 Hz (representing 20% of maximum fan speed) to 60 Hz (representing 100% of maximum fan speed). Both figures show a typical polynomial behavior with power draw increasing with fan speed. These data are used to directly estimate the energy consumption and peak demand of fans in the parking garage model for each control strategy.

4.1 CO concentrations

Figure 15 illustrates a weeklong time-series of spatially averaged time-varying CO concentration results from the CONTAM simulations of the demonstration parking garage for both the majority cold start and majority warm start conditions under both assumptions for traffic schedules. Figure 15(a) and Figure 15(b) show the average CO concentrations (averaged across all zones) assuming Traffic Schedule 1 for the majority cold start and majority warm start conditions, while Figure 15(c) and Figure 15(d) show the average CO concentrations assuming Traffic Schedule 2 for the majority cold start and majority warm start conditions. On the horizontal axes, minute 0 corresponds to 12:00 a.m. on Sunday and minute 10,080 corresponds to 11:59 p.m. on Saturday, with each 1,440-minute interval marking a 24-hour day. Table 2 summarizes the minimum, mean, maximum, and standard deviation of weeklong CO concentrations for each traffic schedule under both engine start condition assumptions and the four control strategies.

The highest and lowest average CO concentrations result from the On-Off strategy and the Always-On strategy, respectively. SVF had the second lowest average CO concentrations, followed by Linear-DCV. Always-On, SVF, and Linear-DCV each maintained peak CO concentrations well below the 1-hour National Ambient Air Quality Standard (NAAQS) limit of 35 ppm in outdoor air in all scenarios (EPA 2019). However, the On-Off strategy consistently exceeded the NAAQS 8-hour average limit of 9 ppm, while the Linear-DCV strategy exceeded the 8-hour limit in only 1 out of 28 total simulation days (EPA 2019). We should note that 1-hour limits are probably a more appropriate comparison than 8-hour limits for human exposure given the short amount of time people spend in parking garages. The differences between the highest peak of spatially averaged CO concentrations for the majority cold start and majority warm start conditions for both

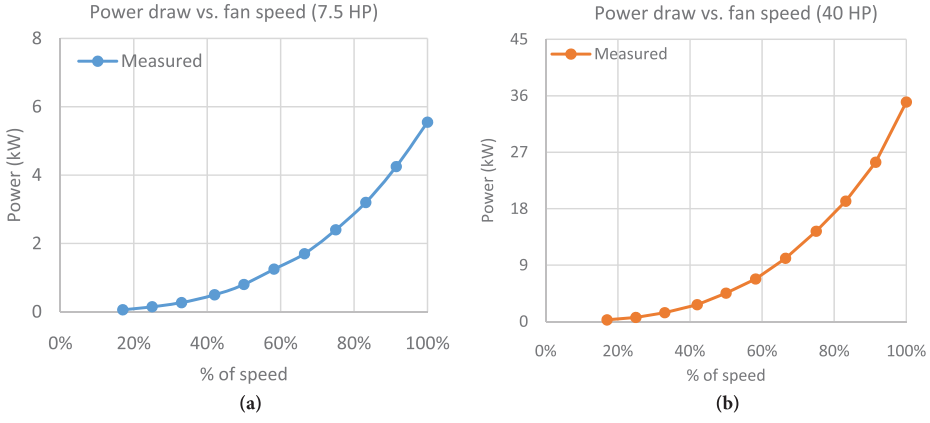

Fig. 14 Measured power draw with respect to fan motor speed: (a) 7.5 HP and (b) 40 HP fans

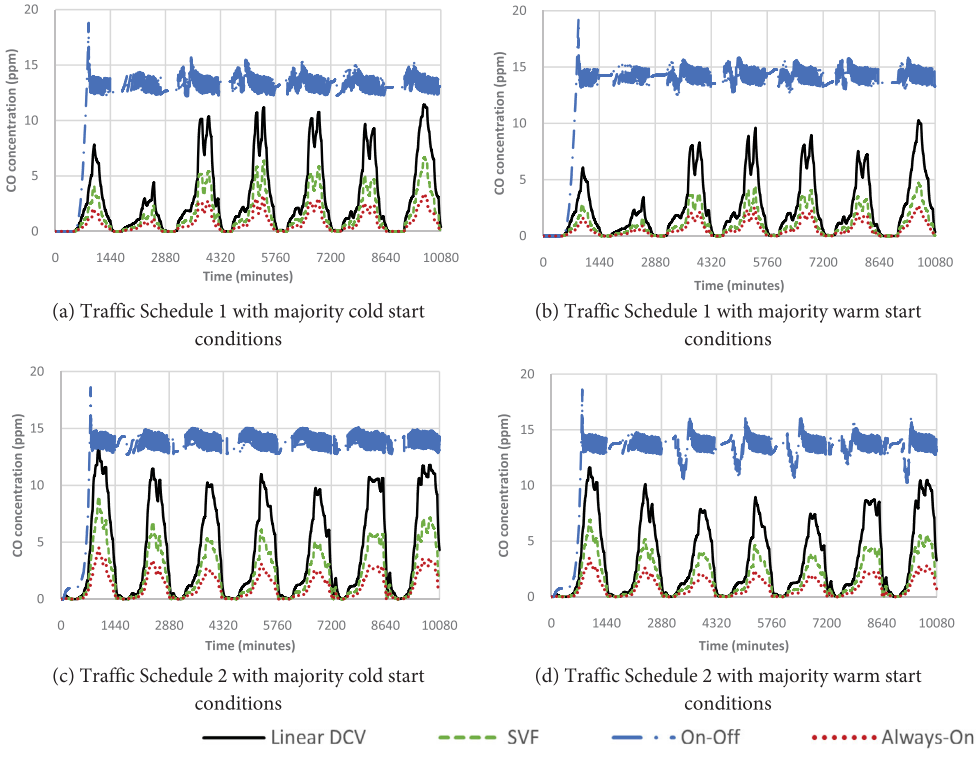

(a) Traffic Schedule 1 with majority cold start conditions

(b) Traffic Schedule 1 with majority warm start conditions

(c) Traffic Schedule 2 with majority cold start conditions

(d) Traffic Schedule 2 with majority warm start conditions

Fig. 15 Weeklong time-series of spatially-averaged CO concentrations in the demonstration parking garage assuming: (a) Traffic Schedule 1 under majority cold start conditions; (b) Traffic Schedule 1 under majority warm start conditions; (c) Traffic Schedule 2 under majority cold start conditions; and (d) Traffic Schedule 2 under majority warm start conditions

Table 2 Summary of weekly-average CO concentrations in each garage for each control strategy and start condition scenario

Traffic Schedule 1 with majority cold start conditions					Traffic Schedule 1 with majority warm start conditions				
CO concentration (ppm)	Linear-DCV	SVF	On-Off	Always-On	CO concentration (ppm)	Linear-DCV	SVF	On-Off	Always-On
Min	0	0	0	0	Min	0	0	0	0
Average	2.97	1.50	12.37	0.75	Average	2.42	1.07	13.17	0.60
Max	11.43	6.69	18.79	3.35	Max	10.26	4.71	19.24	2.65
Std	3.27	1.70	3.39	0.86	Std	2.61	1.18	3.63	0.67
Traffic Schedule 2 with majority cold start conditions					Traffic Schedule 2 with majority warm start conditions				
CO concentration (ppm)	Linear-DCV	SVF	On-Off	Always-On	CO concentration (ppm)	Linear-DCV	SVF	On-Off	Always-On
Min	0	0	0	0	Min	0	0	0	0
Average	4.15	2.18	12.92	1.09	Average	3.37	1.70	12.74	0.85
Max	13.10	8.96	18.62	4.49	Max	11.60	6.90	18.61	3.46
Std	4.16	2.28	3.23	1.15	Std	3.40	1.75	3.32	0.88

schedules ranged from less than 15% on weekends to as much as 25% on weekdays. The reason is not only because of the higher number of outgoing cars in the garage on weekdays, but also due to the sudden peak of outgoing cars at specific times of those days.

4.2 Airflow rates

Figure 16 first shows time-series of the resulting airflow rates associated with each control strategy in the demonstration parking garage using Traffic Schedule 1, adding airflow rates from both the 7.5 and 40 HP fans together. In order to clearly compare the results, the four control strategies are split in two separate panels: Linear-DCV and SVF in one panel and On-Off and Always-On in another panel. Figure 16(a) indicates that the Linear-DCV strategy operates at its minimum setting (i.e., 25% of maximum fan speed) for the majority of the time, except for brief periods, e.g. on

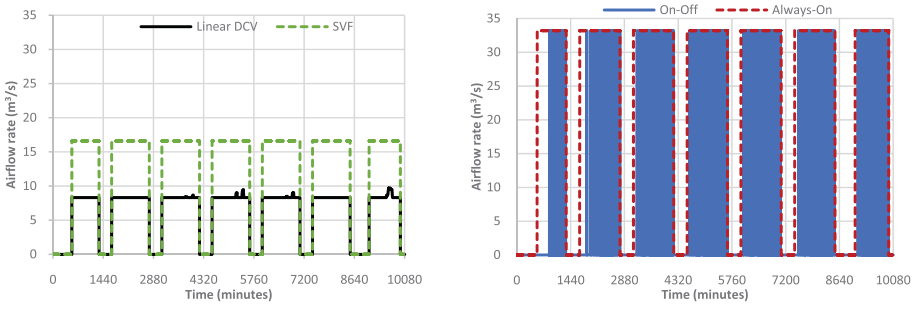

(a) Traffic Schedule 1 with majority cold start conditions

(b) Traffic Schedule 1 with majority cold start conditions

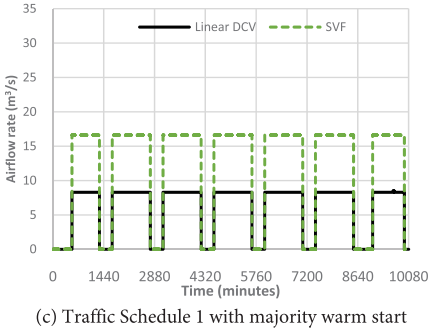

(c) Traffic Schedule 1 with majority warm start conditions

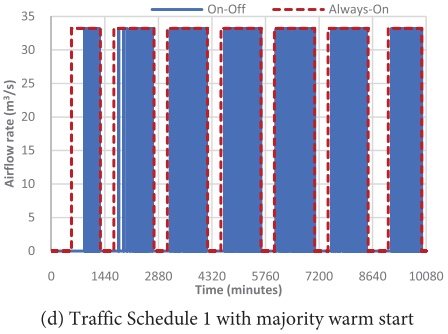

(d) Traffic Schedule 1 with majority warm start conditions

Fig. 16 Time-series of simulated airflow rates in the demonstration parking garage assuming Traffic Schedule 1 for majority cold and warm start conditions

Wednesday, Thursday, and Saturday, when there are a few small jumps, indicating the ramping up and down of fan speeds. These small deviations beyond the baseline resemble the pattern of predicted CO concentrations above 10 ppm shown in Figure 15(a). Conversely, since the SVF strategy fans continuously operating at 50% of maximum capacity when CO concentrations are less than 25 ppm threshold, for this case study there is no increase in motor speed and airflow beyond the 50% of the fan capacity in SVF strategy. As mentioned previously, the airflow associated with full fan capacity for both fans operating together is approximately 33 m^3/s.

In the Always-On strategy, regardless of the CO concentration, the fans are continuously working at full motor capacity. Conversely, in the On-Off strategy, fan operation is simulated to be highly cyclical, which in practice would result in too many signals being sent to actuators to turn the fans on and off. One problem associated with centrifugal fans in an On-Off strategy like this is that during every start-up and shut-down of the fan, the fan blades are subjected to centrifugal, bending, and vibratory loads which finally can reduce the life expectancy of fan blades due to fatigue failure (Dadhich et al. 2015).

Comparing between strategies in Figure 16(a) and Figure 16(b), the Linear-DCV strategy requires the least amount of airflow compared to the others while keeping average CO concentrations well below the defined 25 ppm threshold at all times. The peak airflow rate of the Linear-DCV control strategy, shown in Figure 16(a), occurred during minute 9,656 (on a Saturday) with 9.73 m^3/s (20,620 cfm), which is only ~58% and ~29% of the airflow rate estimated with the SVF and Always-On or On-Off strategies, respectively.

Using Traffic Schedule 1 with the Linear-DCV control under majority warm start conditions, there are only a limited number of times in which the airflow rate is beyond the minimum of 8.25 m^3/s (17,500 cfm) (25%) because of the warm start conditions combined with relatively low occupancy of Traffic Schedule 1 (Figure 16(c)). Thus, it is possible to infer that in warm start condition in this garage, the airflow rate associated with 25% of maximum fan speed is nearly sufficient for diluting the CO level and bringing enough fresh air into the garage. It is expected that SVF would work in its defined based line (50%) as well. In the On-Off strategy depicted in Figure 16(d), there is less frequency of start-up and shut-down of fan due to warm start conditions and lower CO emission rates. In addition, Figure S1 in the Electronic Supplementary Material shows the airflow rate results under Traffic Schedule 2 with both majority cold and warm start conditions.

4.3 Fan power draw and peak demand

Figure 17 and Figure S2 (in the Electronic Supplementary Material) show time-series of the calculated fan power

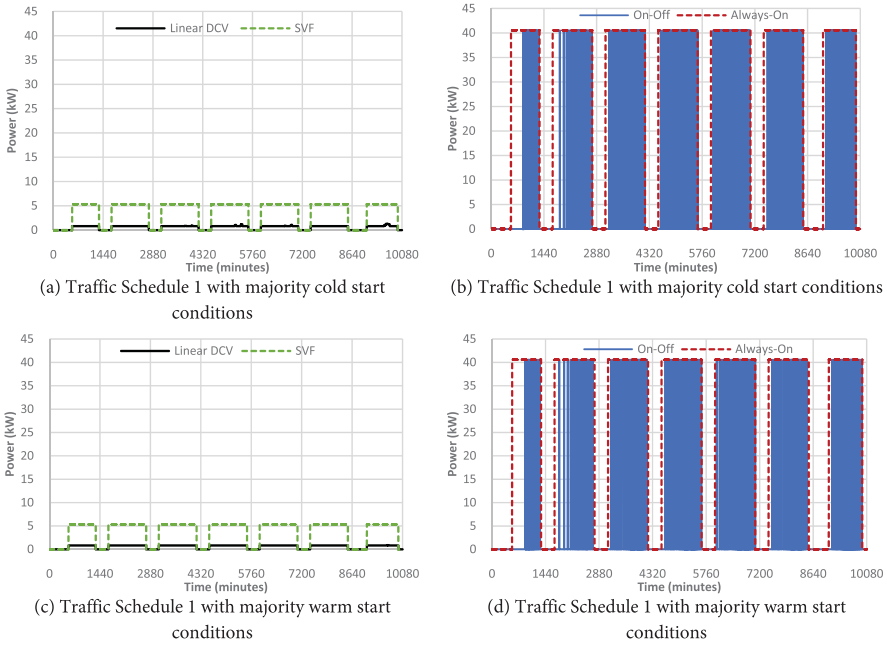

(a) Traffic Schedule 1 with majority cold start conditions

(b) Traffic Schedule 1 with majority cold start conditions

(c) Traffic Schedule 1 with majority warm start conditions

(d) Traffic Schedule 1 with majority warm start conditions

Fig. 17 Calculated fan power draw in the demonstration parking garage assuming Traffic Schedule 1 for majority cold and warm start conditions

draw in the demonstration parking garage for all traffic patterns, control strategies, and engine start scenarios. Similar to the fan airflow figures, fan power draw results are separated by traffic schedule assumption for convenient comparison. Using Traffic Schedule 1 with Linear-DCV in majority cold start conditions (Figure 17(a)), the peak fan power demand was 1.32 kW, occurring in minute 9,656, which is ~76% and ~97%% lower than the peak demand of the SVF and Always-On strategies, respectively (Figure 17(a) and Figure 17(b)). Similarly, using Traffic Schedule 2 under majority cold start conditions, the peak power demand of 2.11 kW occurred in minute 1,010 (a Sunday), which is ~61% and ~95% lower than the peak power demand by SVF and Always-On strategies, respectively. Figure 17(c) and Figure 17(d) show that in the majority warm start conditions using Traffic Schedule 1, the Linear-DCV and SVF strategies did not draw more power than the baseline operating conditions.

Table 3 summarizes distributions of fan power demand results for both traffic assumptions and all emission and control scenarios, including both the power draw (or ranges of power draws for variable speed systems) and the duration of those power demands. The duration and its associated binned range of power demand in Table 3 shows for how many minutes a fan draws how much power. For example, for Traffic Schedule 1 with majority warm start conditions, during the weeklong period Linear-DCV fans draw between 0.83 kW and 0.9 kW for a total of 52 minutes. Ranges of power draw are shown because fan power draw is variable based on demand; thus, power draw variations are binned within specific ranges for clarity. The Linear-DCV strategy is predicted to have a much lower peak power draw than other strategies because of its low baseline fan speed and Linear response of the fan speed to CO concentrations. The average and standard deviation reduction in peak demand achieved by the Linear-DCV strategy, averaged across all conditions, is estimated to be ~78.2%±5.1%, ~97.1%±0.7%, and ~97.1%±0.7% compared to the SVF, On-Off, and Always-On strategies, respectively.

4.4 Fan energy use

Table 4 summarizes the estimated annual fan energy consumption for the demonstration parking garage using the two traffic schedules, two engine start scenarios, and four different ventilation control strategies, assuming the one-week simulation results shown previously also represent all 52 weeks of the year. Actual fan energy use will vary weekly and seasonally depending on occupancy patterns, but this simplifying assumption allows for a reasonable extrapolation to an entire year for the purposes of comparison.

Similarly, Table 5 presents the percent fan energy savings predicted with the Linear-DCV control strategy compared to other baseline strategies. The Linear-DCV control strategy consistently resulted in the lowest fan energy usage, providing an average (standard deviation) savings across all scenarios of ~97.9%±0.1%, ~85.3%±2.3%, and ~72.8%±3.6% compared to the Always-On, SVF, and On-Off strategies, respectively.

Table 3 Distributions of estimated fan power demand and duration for the demonstration parking garage assuming each traffic schedule, engine start scenario, and control strategy

Linear-DCV		SVF		On-Off		Always-On	
Duration (min)	Demand (kW)	Duration (min)	Demand (kW)	Duration (min)	Demand (kW)	Duration (min)	Demand (kW)
Traffic Schedule 1 fans with majority warm start conditions							
52	0.83–0.9	—	—	—	—	—	—
7,021	0.82	7,073	5.34	427	40.55	7,073	40.55
3,008	0	3,008	0	9,654	0	3,008	0
Traffic Schedule 2 fans with majority warm start conditions							
397	0.83–0.97	—	—	—	—	—	—
8,447	0.82	8,904	5.34	649	40.55	8,904	40.55
1,177	0	1,177	0	9,432	0	1,177	0
Traffic Schedule 1 fans with majority cold start conditions							
476	0.83–1.32	—	—	—	—	—	—
6,599	0.82	7,073	5.34	570	40.55	7,073	40.55
3,006	0	3,008	0	9,511	0	3,008	0
Traffic Schedule 2 fans with majority cold start conditions							
1,556	0.83–2.12	—	—	—	—	—	—
7,348	0.82	8,904	5.34	823	40.55	8,904	40.55
1,177	0	1,177	0	9,258	0	1,177	0

Table 4 Annual ventilation fan energy consumption for the demonstration parking garage using two traffic schedules, two engine start scenarios, and four control strategies

	Estimated total annual fan energy consumption (kWh)			
	Majority warm start conditions		Majority cold start conditions	
Control strategy	Traffic Schedule 1	Traffic Schedule 2	Traffic Schedule 1	Traffic Schedule 2
Linear-DCV	5,028	6,387	5,114	6,769
SVF	32,734	41,208	32,734	41,208
On-Off	15,809	22,808	20,032	28,923
Always-On	248,569	312,916	248,569	312,916

Table 5 Annual fan energy savings of the Linear-DCV strategy compared to three industry-standard control strategies for two traffic schedules and two engine start scenarios

Linear-DCV savings compared to other control strategies	Estimated total annual fan energy savings (%)			
	Majority warm start conditions		Majority cold start conditions	
	Traffic Schedule 1	Traffic Schedule 2	Traffic Schedule 1	Traffic Schedule 2
vs. SVF	84.6%	84.5%	84.4%	83.6%
vs. On-Off	68.2%	72.0%	74.5%	76.6%
vs. Always-On	98.0%	98.0%	97.9%	97.8%

4.5 Electricity cost and payback period

The aim of this section is to estimate the annual electricity cost of each control strategy for the demonstration parking garage case study and calculate the payback period of installation of VFDs in the Linear-DCV strategy compared to other control strategies. To estimate annual energy costs, we used Time-of-Use (TOU) electricity rates and schedules from Pacific Gas and Electric (PGE), which is the utility provider in San Francisco, CA (PG&E 2020b), as shown in Table 6. We did not consider variations in peak demand charges since the size of fans are less than 75 kW. We

Table 6 TOU program for summer and winter time in San Francisco

		Peak	Partial-peak	Off-peak
Summer	Hours	12:00 noon to 6:00 pm	8:30 a.m. to 12:00 noon and 6:00 p.m. to 9:30 p.m.	9:30 p.m. to 8:30 a.m.
	Days	Monday through Friday	Monday through Friday	All days
	Rate ($ per kWh)	0.29592	0.27227	0.24491
Winter	Hours	—	8:30 a.m. to 9:30 p.m.	9:30 p.m. to 8:30 a.m.
	Days	—	Monday through Friday	All days
	Rate ($ per kWh)	—	0.25166	0.23075

considered electricity rates with and without rebates of $80 per HP currently offered for the fan upgrades (PG&E 2020a).

The estimated annual cost of energy use is shown in Table 7. Similar to prior assumptions without TOU pricing, the Linear-DCV strategy shows large cost savings compared to the other three strategies.

To estimate upfront installation costs of VFDs and the resulting simple payback period, we used real project installation costs of $75,000, which we obtained from the actual project contractor. Upfront costs include the costs of (i) project design, logistical management, installation & system commissioning, (ii) all CO sensors, (iii) controller JACE, (iv) Danfoss FC100 VLT VFDs, (v) RS485 repeater, and (vi) equipment start-up. Detailed installation costs were not available for the SVF or On-Off strategies, but they would also require adding VFDs, system design, installation, and automation costs. Table 8 shows the estimated simple payback periods of installing VFDs and operating the Linear-DCV strategy compared to the Always-On strategy (without VFDs) for the demonstration case study, both with and without fan rebates.

The estimated simple payback period for the system design and installation of the Linear-DCV strategy ranged from 11.7 to 14.5 months without rebates, with an average of 13.1 months, and from 11.2 to 13.7 months with rebates, with an average of 12.4 months. The estimated payback periods in all cases are notably lower than the common practice of a three-year payback period for energy efficiency measures (EEMs).

5 Discussion

To the knowledge of the authors, this is one of the first comprehensive studies to assess the energy use and peak power demand associated with different types of control strategies in underground parking garages while maintaining acceptable levels of indoor air quality. Previous studies either did not consider complex control strategies and/or dated back to times when average CO emission rates

Table 7 Annual energy cost for the demonstration parking garage using two traffic schedules, two engine start scenarios, and four control strategies

	Estimated total annual cost ($)			
	Majority warm start conditions		Majority cold start conditions	
Control strategy	Traffic Schedule 1	Traffic Schedule 2	Traffic Schedule 1	Traffic Schedule 2
Linear-DCV	1,278	1,601	1,299	1,694
SVF	8,319	10,334	8,319	10,334
On-Off	3,879	5,809	5,185	7,372
Always-On	63,171	78,476	63,171	78,476

Table 8 Payback period of Linear-DCV strategy compared to Always-On control strategy for two traffic schedules and two engine start scenarios

Linear-DCV strategy compared to Always-On strategy	Estimated payback period (months)			
	Majority warm start conditions		Majority cold start conditions	
	Traffic Schedule 1	Traffic Schedule 2	Traffic Schedule 1	Traffic Schedule 2
Without rebate	14.5	11.7	14.5	11.7
With rebate	13.7	11.2	13.7	11.2

of internal combustion engine vehicles were higher. Developments in engines as well as ventilation control hardware and software can allow for more sophisticated fan controls that can save energy and reduce peak demand.

One important outcome of this study is to demonstrate that although the On-Off option strategy provides significant energy savings compared to Always-On or SVF, it does not address the peak demand savings and leads to high CO concentrations as modeled. Conversely, the Linear-DCV strategy reduces peak demand substantially in addition to providing electricity savings and maintaining CO concentrations below defined threshold values. This strategy has implications for locations where utility providers offer various Demand Response (DR) or TOU programs, as described in Section 4.5. It is also important to note that none of the strategies led to garage CO concentrations that exceeded permissible limits.

One important factor in developing DCV-based ventilation control strategies is to determine how a collection of fans in an underground parking garage operate. Depending on the design and size of an underground parking garage, there might be a need to install dozens of fans. In developing control strategies, one might apply any of the discussed control strategies per fan and/or per zone, meaning each fan decides based on the zone concentration. However, one might assume that each fan receives the same control signal and once a zone detects a high CO level, all the fans operate in the same manner. This collective decision also opens up the possibility to seek an optimal fan control strategy. The results of this study show that if the decision-making is based on the average CO level of the zones, there are only a few hours that require more fan airflow than the baseline levels in the Linear-DCV-based control strategy, as modeled.

It is also important to select the minimum airflow rate to meet the local building jurisdiction, which will affect the minimum fan speeds and power draws for any demand-based strategy. Since the case study parking garage is located in California, the minimum fan speed was defined to meet the Title 24's minimum airflow rate. Additionally, the On-Off control strategy as defined does not meet the minimum airflow rate requirement of 0.75 L/(s·m^2) in California. However, it is included to demonstrate an extreme case that is used elsewhere. We acknowledge that consideration of different minimum fan speeds would yield different energy, peak demand, and cost savings. Therefore, adopting the strategies proposed in this paper requires ensuring the minimum airflow is provided when a parking garage is in operation, which may vary by location.

In addition, the lower range of the current Linear-DCV-based control strategy is based on limitations of VFD motors. VFD motors usually cannot operate in frequencies lower than 10 Hz. It is also possible to benefit from Variable Speed Drives (VSDs) to decrease the motor speed to less than 10%, meaning the lower limit of the CO level could also be different. Therefore, future studies can assess these factors in their decision-making. Last, as cold start CO emission rates of vehicles continue to decline (EPA 2015) and as electric vehicles (EVs) continue to grow in market share, future studies of parking garage ventilation controls and pollutant concentrations should continue to incorporate updated assumptions for tailpipe emission rates. Overall, although a large number of existing parking garages do not benefit from a DCV strategy to reduce energy and peak demand, based on the savings predicted herein, retrofits of existing underground parking garages should prioritize adding controllers to utilize DCV strategies.

6 Conclusion

This study developed and applied a simulation framework for investigating the impact of various ventilation controls strategies on indoor air quality and fan energy use in parking garages using a multi-zone airflow and contaminant transport modeling tool (CONTAM). Four different ventilation control strategies were evaluated in a validated case study, including three strategies commonly used in the industry (On-Off, Always-On, and Standardized Variable Flow (SVF)), and one more recently developed strategy (Linear-Demand Controlled Ventilation (DCV)). Under a variety of assumptions for model input parameters, the modeling approach predicts that each ventilation strategy succeeds in maintaining average CO concentrations below defined threshold values, although the Always-On strategy maintained the lowest CO concentrations, followed by SVF, Linear-DCV, and On-Off, respectively. The estimated annual average fan energy consumption was consistently lowest with the Linear-DCV strategy, resulting in average energy savings (± standard deviation) of 84.3%±0.4%, 72.8%±3.6%, and 97.9%±0.1% compared to SVF, On-Off and Always-On strategies, respectively, averaged across all modeled scenarios. Moreover, the peak electricity demand using the Linear-DCV strategy was, on average, ~20% of the peak demand using the SVF strategy and only ~3% of the On-Off or Always-On control methods, respectively. The average estimated simple payback period for the Linear-DCV compared to the Always-On strategy was around 13 months, which is considerably lower than the common assumption of a three-year payback period for energy efficiency measures (EEMs). The results of this study have direct implications for improving existing controls in building automation systems, not only in parking garages but in other building types as well. Moreover, the utility of the framework described herein is that it can be used to

model energy and indoor air quality impacts of other parking garage configurations and control scenarios.

Acknowledgements

This work was supported by Nagle Energy Solutions, LLC, which provided empirical data utilized in this study. The authors would like to thank Frank Nagle and Ron Lea for their guidance throughout this project and paper preparation. This study was funded in part by an ASHRAE New Investigator Award to Mohammad Heidarinejad and an ASHRAE Graduate Grant-In-Aid to Afshin Faramarzi.

Electronic Supplementary Material (ESM): supplementary material is available in the online version of this article at https://doi.org/10.1007/s12273-020-0677-3.

References

Abdel-Rahman AA (1998). On the emissions from internal-combustion engines: A review. *International Journal of Energy Research*, 22: 483–513.

ACGIH (1998). Industrial Ventilation: A Manual of Recommended Practice, 23rd edn. American Conference of Governmental Industrial Hygienists.

Aminian J, Maerefat M, Heidarinejad G (2018a). A new simplified method for decreasing contaminants in underground enclosed parking lots. *Building Services Engineering Research and Technology*, 39: 590–608.

Aminian J, Maerefat M, Heidarinejad G (2018b). The enhancement of pollutant removal in underground enclosed parking lots by reconsideration of the exhaust vent heights. *Tunnelling and Underground Space Technology*, 77: 305–313.

ASHRAE (2008). ASHRAE Handbook—HVAC Systems and Equipment. Atlanta, GA, USA: American Society of Heating, Refrigerating and Air-Conditioning Engineers.

ASHRAE (2011). ASHRAE Handbook. HVAC Applications: Chapter 15: Enclosed Vehicular Facilities. Atlanta, GA, USA: American Society of Heating, Refrigerating and Air-Conditioning Engineers.

ASHRAE (2017). ASHRAE Handbook of Fundamentals. Atlanta, GA, USA: American Society of Heating, Refrigerating and Air-Conditioning Engineers.

ASHRAE (2019). Standard 62.1-2019, Ventilation for Acceptable Indoor Air Quality. Atlanta, GA, USA: American Society of Heating, Refrigerating and Air-Conditioning Engineers.

Ayari AM, Grot DA, Krarti M (2000). Field evaluation of ventilation system performance in enclosed parking garages. *ASHRAE Transactions*, 106(1): 228–237.

Bielaczyc P, Szczotka A, Woodburn J (2013). An overview of cold start emissions from direct injection spark-ignition and compression ignition engines of light duty vehicles at low ambient temperatures. *Combustion Engines*, 154(3): 96–103.

CARB (1997). Methodology for calculating and redefining cold and hot start emissions. Available at https://ww3.arb.ca.gov/msei/onroad/downloads/pubs/starts.pdf

CARB (2017a). An Update to California On-Road Mobile Source Emission Inventory. EMFAC2017 Workshop. Available at https://www.arb.ca.gov/msei/downloads/emfac2017_workshop_june_1_2017_final.pdf

CARB (2017b). EMFAC2017 User's Guide. California Air Resources Board Mobile Source Analysis Branch. Available at https://www.arb.ca.gov/msei/downloads/emfac2017_users_guide_final.pdf

Chan MY, Burnett J, Chow WK (1998). Energy use for ventilation systems in underground car parks. *Building and Environment*, 33: 303–314.

Chan MY, Chow WK (2004). Car park ventilation system: Performance evaluation. *Building and Environment*, 39: 635–643.

Cho H-J, Jeong W (2013). Energy saving potentials of demand-controlled ventilation based on real-time traffic load in underground parking facilities. In: Proceedings of Building Solutions for Architectural Engineering (AEI 2013).

Dadhich M, Kumar Jain S, Sharma V, Kumar Sharma S, Agarwal D (2015). Fatigue (FEA) and modal analysis of a centrifugal fan. *International Journal of Recent Advances in Mechanical Engineering*, 4(2): 77–91.

Demetriou DW, Khalifa HE (2009). Evaluation of distributed environmental control systems for improving IAQ and reducing energy consumption in office buildings. *Building Simulation*, 2: 197–214.

Dols WS, Polidoro BJ (2015). CONTAM user guide and program documentation. NIST Technical Note 1887. Gaithersburg, MD, USA: National Institute of Standards and Technology.

Dols WS, Emmerich SJ, Polidoro BJ (2016). Coupling the multizone airflow and contaminant transport software CONTAM with EnergyPlus using co-simulation. *Building Simulation*, 9: 469–479.

Duci A, Papakonstantinou K, Chaloulakou A, Markatos N (2004). Numerical approach of carbon monoxide concentration dispersion in an enclosed garage. *Building and Environment*, 39: 1043–1048.

Emmerich SJ, Dols WS (2016). Model validation study of carbon monoxide transport due to portable electric generator operation in an attached garage. *Journal of Building Performance Simulation*, 9: 397–410.

Emmerich SJ, Polidoro BJ, Dols WS (2016). Simulation of residential carbon monoxide exposure due to generator operation in enclosed spaces. NIST Technical Note 1925. Gaithersburg, MD, USA: National Institute of Standards and Technology.

EPA (2000). Air Quality Criteria for Carbon Monoxide (EPA 600/P-99/001F). U.S. Environmental Protection Agency.

EPA (2015). Exhaust Emission Rates for Light-Duty on-road Vehicles in MOVES2014 (EPA-420-R-15-005). U.S. Environmental Protection Agency.

EPA (2019). National Ambient Air Quality Standards (NAAQS). Criteria Air Pollutants. U.S. Environmental Protection Agency. Available at https://www.epa.gov/criteria-air-pollutants/naaqs-table

Gao HO, Johnson LS (2009). Methods of analysis for vehicle soak time data. *Transportation Research Part A: Policy and Practice*, 43: 744–754.

Gil-Lopez T, Sanchez-Sanchez A, Gimenez-Molina C (2014). Energy, environmental and economic analysis of the ventilation system of enclosed parking garages: Discrepancies with the current regulations. *Applied Energy*, 113: 622–630.

Guyot G, Sherman MH, Walker IS (2018). Smart ventilation energy and indoor air quality performance in residential buildings: A review. *Energy and Buildings*, 165: 416–430.

Hesaraki A, Holmberg S (2015). Demand-controlled ventilation in new residential buildings: Consequences on indoor air quality and energy savings. *Indoor and Built Environment*, 24: 162–173.

Hong T, Fisk WJ (2010). Assessment of energy savings potential from the use of demand controlled ventilation in general office spaces in California. *Building Simulation*, 3: 117–124.

ICC (2015). International Mechanical Code (IMC). International Code Council (ICC).

Krarti M, Ayari A, Grot D (1998). ASHRAE 945-RP: Evaluation of Fixed and Variable Rate Ventilation System Requirements for Enclosed Parking Facilities. Atlanta, GA, USA: American Society of Heating, Refrigerating and Air-Conditioning Engineers.

Krarti M, Ayari A (2003). CFD analysis of ventilation system performance for enclosed parking garages. *ASHRAE Transactions*, 109(2): 455–469.

Laverge J, van den Bossche N, Heijmans N, Janssens A (2011). Energy saving potential and repercussions on indoor air quality of demand controlled residential ventilation strategies. *Building and Environment*, 46: 1497–1503.

Liu Z, Yin H, Ma S, Jin G, Gao J, Ding W (2019). On-site assessments on variations of $PM_{2.5}$, PM_{10}, CO_2 and TVOC concentrations in naturally ventilated underground parking garages with traffic volume. *Environmental Pollution*, 247: 626–637.

Lorenz F (1982). Calculation of ventilation requirements in the case of intermittent pollution: Application to enclosed parking garages. *Environment International*, 8: 515–524.

Lu T, Lü X, Viljanen M (2011). A novel and dynamic demand-controlled ventilation strategy for CO_2 control and energy saving in buildings. *Energy and Buildings*, 43: 2499–2508.

Marr LC, Morrison GC, Nazaroff WW, Harley RA (1998). Reducing the risk of accidental death due to vehicle-related carbon monoxide poisoning. *Journal of the Air & Waste Management Association*, 48: 899–906.

NES (2020). NES Series 200 Carbon Monoxide (CO) RS-485 Transmitters. Available at https://www.nagleenergy.com/wp-content/uploads/2015/02/Product-Specifications-%E2%80%93-NES-200-CO-Modbus.pdf

OSHA (2012). OSHA Fact Sheet: Carbon Monoxide Poisoning. Occupational Safety and Health Administration. Available at https://www.osha.gov/OshDoc/data_General_Facts/carbonmonoxide-factsheet.pdf

PG&E (2020a). Business Rebate Catalog. Pacific Gas and Electric Company. Available at https://www.pge.com/pge_global/common/pdfs/save-energy-money/business-solutions-and-rebates/product-rebates/business-rebate-catalog.pdf

PG&E (2020b). Pacific Gas and Electric Company: Electric Schedule A-1 Small General Service. Available at https://www.pge.com/tariffs/assets/pdf/tariffbook/ELEC_SCHEDS_A-1.pdf

Qi D, Wang L, Zmeureanu R (2015). Modeling smoke movement in shafts during high-rise fires by a multizone airflow and energy network program. *ASHRAE Transactions*, 121(2): 242–251.

Title 24 (2013). California Code for Regulations Title 24: Section 120.6(c) Part 6: Mandatory Requirements for Enclosed Parking Garages. California Energy Commission. https://ww2.energy.ca.gov/2012publications/CEC-400-2012-004/CEC-400-2012-004-CMF-REV2.pdf

Wang L, Emmerich SJ, Lin C-D (2014). Study of the impact of operation distance of outdoor portable generators under different weather conditions. *Indoor and Built Environment*, 23: 1092–1105.

Zhao Y, Song X, Wang Y, Zhao J, Zhu K (2017). Seasonal patterns of PM_{10}, $PM_{2.5}$, and $PM_{1.0}$ concentrations in a naturally ventilated residential underground garage. *Building and Environment*, 124: 294–314.

Zhao Y, Wang Y, Zhu K, Zhao J (2018). Seasonal variations and exposure levels of carbon monoxide in a naturally ventilated residential underground parking lot. *Science and Technology for the Built Environment*, 24: 73–82.